Lab on a Chip

PAPER

View Article Online
View Journal | View Issue

Cite this: *Lab Chip*, 2021, **21**, 2272

Implementation of iMiDEV™, a new fully automated microfluidic platform for radiopharmaceutical production†

Olga Ovdiichuk, [a] Hemantha Mallapura,[b] Florian Pineda,[c] Virginie Hourtané,[c] Bengt Långström,[d] Christer Halldin,[b] Sangram Nag,[b] Fatiha Maskali,[a] Gilles Karcher[ae] and Charlotte Collet *[af]

Received 24th February 2021,
Accepted 21st April 2021

DOI: 10.1039/d1lc00148e

rsc.li/loc

iMiDEV™ microfluidic system is a new automated tool for a small-scale production of radiopharmaceuticals. This new radiochemistry module utilizes microfluidic cassettes capable of producing diversified radiopharmaceuticals in liquid phase reactions in an automated synthesizer. The user interface is intuitive and designed to give the operator all the information required and to allow driving the synthesis either manually or fully automatically. In this work, we have demonstrated liquid phase reaction and presented the first results of an efficient fully automated [^{18}F]NaF radiosynthesis on the iMiDEV™ platform. Different parameters such as a type of cyclotron targets, initial activity, concentration and volume of the fluoride-18 targetry have been investigated in order to elaborate the optimised radiolabelling of the ligand. Single and double sodium [^{18}F]fluoride synthesis procedures have been successfully developed using two chambers of the cassette. A single-dose of radiotracer was produced in an average radiochemical yield of 87% (decay corrected) within 8 min and quality control tests were performed as per European Pharmacopoeia.

1 Introduction

Positron emission tomography (PET) is an important medical imaging technique that relies upon uses of radioactive molecules for *in vivo* visualisation of a variety of physiological and pathophysiological processes in human body. These specific molecules, also called tracers or radiopharmaceuticals, are labelled with positron emitting radionuclide, such as ^{18}F, ^{11}C or ^{68}Ga. Tracers provide the information necessary for diagnosis and staging of diseases, treatment selection and guidance as well as for PET-guided radiotherapy as theranostic probes.[1,2] Their development is conducted by big radiopharmaceutical production centres in a shielded cell using large-scale automated synthesis units connected to the cyclotron. Drawbacks of such production include huge investments in the infrastructure, radioactivity loss due to long delivery time and related to them limited availability of specialized tracers and their expensive cost. To overcome these disadvantages and to provide a wider access to PET imaging agents through dose-on-demand synthesis, microfluidic systems have been developed. Since 2007 researchers were trying to respond to the question "Whether microfluidics are a breakthrough technology, a golden opportunity for the microscale PET tracer production?"[3–5] At present, numerous tracers have been successfully produced using different microfluidic systems.[6] The benefits of these systems include high surface-to-volume ratio and heat transport which increase the reaction rate and decrease consumption of reagents due to small reaction volumes. Overall, this allows better optimisation and miniaturisation of a tracer production and thereby reduces its cost. Moreover, contrary to the commercial facilities producing common tracers, such as widespread tracer [^{18}F]FDG, which are not necessarily close to clinical and research sites, microfluidic technology stand for decentralized dose-on-demand (DOD) production of diverse PET probes.[7–9] In the perspective of DOD production, only the necessary amount of radioactivity for the injection to one patient after quality control is used. This brings another advantage which is an opportunity to produce tracers labelled with short-lived radionuclides, such as carbon-11 (half-life of 20.4 minutes).[10,11]

[a] *Nancyclotep, Molecular Imaging Platform, 5 rue du Morvan, F-54500 Vandoeuvre les Nancy, France. E-mail: c.collet@nancyclotep.com*
[b] *Department of Clinical Neuroscience, Center for Psychiatry Research, Karolinska Institutet and Stockholm County Council, Stockholm 17176, Sweden*
[c] *PMB Alcen, Route des Michels CD56, F-13790 Peynier, France*
[d] *Department of Chemistry, Uppsala University, Sweden*
[e] *CHRU-Nancy, Department of Nuclear Medicine, F-54000, Vandoeuvre les Nancy, France*
[f] *INSERM U1254 IADI, Université de Lorraine, F-54500 Vandoeuvre les Nancy, France*
† Electronic supplementary information (ESI) available. See DOI: 10.1039/d1lc00148e

There are multiple microfluidic systems reported so far for radiotracer production. Depending on the microreactor type microfluidics are classified as follows: (i) continuous flow or microchannel; (ii) batch-type or chamber; (iii) droplet or digital microfluidics. Continuous flow systems consist of channel networks where reagents are mixed and reacted while moving through a serpentine or loop microreactor.[12–14] This technique formed the basis for the commercial Advion Biosciences system "Nanotek" used for the microfluidic synthesis of 34 different tracers.[6,15,16] Batch-type or chamber system can be considered as a miniaturised version of the traditional scale synthesis with all benefits of microfluidics and relatively simple transfer from the conventional procedure to the microscale process and automation.[17–19] Droplet microfluidics manipulate droplets as microreactors. These systems can be divided into three subtypes: (1) electrowetting-on-dielectric (EWOD) devices in which droplets are generated and manipulated through surface tension;[20,21] (2) systems that leverage a simple passive transport mechanism based on the hydrophobic and hydrophilic properties of the materials of the cassette (chip) to generate droplet movement;[22] (3) magnetic droplet microfluidics (MDM) use magnetic force for the motion of the droplets.[23,24] The main limitation of these systems is to perform all required production steps: radionuclide concentration, labelling, purification and formulation in an injectable solution within a device (on-chip). Therefore, most of the platforms reported so far have modular construction employing microfluidic approach for the labelling step and conventional off-chip modules and consumables are used for other essential steps.[23] However, some progress has been achieved in the development of the fluoride-18 and gallium-68 concentration systems adapted or integrated into microfluidic cassettes.[24–29] Recently, a new custom platform that can perform steps starting from radionuclide concentration and finishing with purification of the final product has been shown to successfully produce a [^{18}F] fallypride dose.[19] Nevertheless, fabrication and industrialisation of a fully integrated on-chip platform remains an engineering challenge of great interest.

Here we present a new fully automated platform for on-cassette PET radiotracer production called iMiDEV™. The developed syntheses will then be used in the fully robotized single-dose radiopharmaceutical production system called iMiLAB™. Both iMiDEV™ and iMiLAB™ systems are based on the same microfluidic technology. [^{18}F]NaF tracer has been chosen for the proof of concept study. This radioligand is known as a bone imaging probe since 1972.[30] A significant increase in [^{18}F]NaF-related publications and studies began in 2011 from the approval by the Food and Drug Administration (FDA) for PET bone scans and has continued since then.[31] Although the automated large-scale production of [^{18}F]NaF is available using existing commercial synthesizers,[32] no microfluidics have been applied to synthesize this radiopharmaceutical so far. In the present work a development of the fully automated single-dose synthesis using different chambers (R1 and R3) of the microfluidic cassette is described. This approach fits perfectly with the main purpose of microfluidics which is decentralized single-dose radiopharmaceutical drug production. Additionally, the subsequent radiosynthesis of two batches of [^{18}F]NaF on the same cassette and without the need of reloading chemicals was explored. Finally, the quality control data of sodium [^{18}F]fluoride produced on the iMiDEV™ fully complies with the most recent European Pharmacopoeia (2020).[33]

2 Experimental

2.1 Chemicals and materials

0.9% Sodium chloride (NaCl) solution for injections was purchased from Baxter®. Distilled, sterile H_2O of pharmaceutical grade was purchased from Dutscher®, France, sterile Millex filters from Millipore® and sterile product vials from Cis-Bio international® (Tec-Elu-5). ^{18}O-enriched water was supplied by CortecNet®. No-carrier-added fluoride-18 was produced *via* the ^{18}O(p,n)^{18}F nuclear reaction on a 16.4 MeV PET Trace cyclotron (General Electric, Connecticut, USA) at the CURIUM™ facility (Nancy, France) and on a GEMS 16.4 MeV PET trace Cyclotron at the Karolinska Institutet PET Centre (Stockholm, Sweden). Glass vials of capacity 4 mL and 15 mL (SCHOTT ISO clear type/tubular) were used with the cassette. All the reagents and materials were used as received.

2.2 iMiDEV™ system description

iMiDEV™ (PMB-ALCEN, France) is an original research and development system for microfluidic chamber type radiotracer production using a novel microfluidic cassette in micro and/or macroscale. The iMiDEV™ system can produce different synthesis in both liquid and gas phase using the same equipment thus allowing us to improve and to develop the radiopharmaceutical DOD production panel. An optimisation of the macro-scale conventional synthesis parameters to the microfluidic technology is necessary to achieve efficient and reliable production process. The iMiDEV™ system consists of several subunits whose functions make it possible to carry out all steps of the syntheses (Fig. 1 and 2).

Docking station (Fig. 1 and 2): it controls the synthesizer. It is the first subsystem connected to a compressed air and the carrier gas (N_2 or He) supplies. A succession of equipment allows these two supplies to be distributed across several pressure-controllable circuits. Compressed air is used to drive pneumatic actuators (valves and clamping system). A series of solenoid valves redistributes the pressure through 44 outlets (10 for clamping and Rheodyne valve and 34 for microfluidic valves). Microfluidic valves are located on the bottom part of the cassette.

Synthesizer called "Box" (Fig. 1 and 2): the carrier gas is injected into the microfluidic network of the cassette placed in the box to move the liquids. The pressure modulation inside the vials containing the reagents is performed by the pressure controller located in the docking station (Fig. 3b).

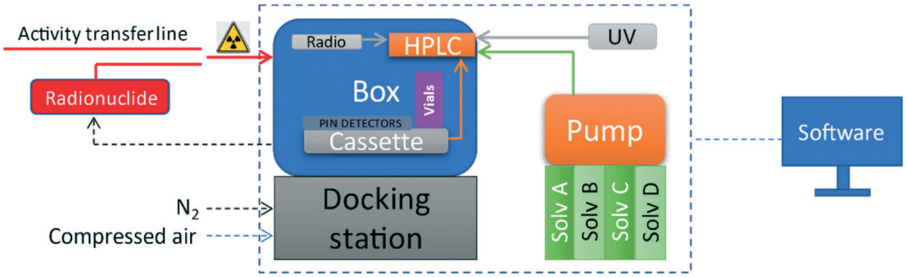

Fig. 1 Schematic of iMiDEV™ system components; box (synthesizer) outer dimensions: 320 mm × 400 mm × 300 mm.

The iMiDEV™ system can be configured in two modes:1) to work with a radionuclide solution in an external vial connected to the cassette through the isotope port; 2) radionuclide is transferred to the cassette *via* a direct line connected to the cyclotron targetry system (Fig. 1).

Additionally, the synthesizer has an HPLC system which is divided into 2 parts: the first is integrated inside the box (2 Rheodyne loops and valves, 1 HPLC column with guard column, a UV cell and radioactivity detector) and the second remote part, outside the box, which consists of UV detector, mobile phase and pumping system (up to 400 bar).

During the synthesis process, activity is measured at 4 different locations in the cassette with 4 positive intrinsic negative (PIN) diode radiation detectors (2.7 × 2.7 mm^2) whose range of measurement is between 37 MBq – 37 GBq (1 and 1000 mCi). The detectors are located inside the box in front of each chamber (Fig. 1).

The reagents can be heated up to 130 °C in the R2 reaction chamber of the microfluidic cassette, thanks to a thermoelectric device composed of 2 Peltier elements.

2.3 iMiDEV microfluidic cassette

Batches of iMiDEV microfluidic cassettes were fabricated by MiniFAB (Australia). This cassette is divided in 2 parts: the vial holder and the microfluidic circuit (Fig. 3a).[34] The first part is used to maintain vials filled with reagents on top of spikes (Fig. 3b). In the microfluidic circuit, channels are present on the top and the bottom side. The channel and mixer dimensions are provided in ESI† Table S1. The cassette is made of cyclic olefin polymer (COP 1430R) which is usually used for microfluidic and medical applications. COP is compatible with many reagents utilized in radiochemistry and with heating process up to 150 °C. COC-E-140 membrane at 100 μm thickness was used for the 34 microfluidic valves formation that replace traditional stopcock valves and to seal the channels on the bottom layer. The unique architecture of the cassette was designed based on main steps to achieve a microscale version of the conventional automated radiosynthesis. In contrast to majority of existing chamber-based microfluidic devices designed for dose-on-demand radiopharmaceutical production, iMiDEV™ cassette is a multifunctional tool that enables not only to move and to mix liquids but also: i) to conduct reactions in a liquid phase and/or on the solid phase support; ii) radioactivity concentration; iii) solid phase extraction (SPE) purification and formulation within the cassette; iv) possibility to connect to the HPLC loops and purification column. While reactor R2 is an open liquid reactor designed to be filled with up to 300 μL, in solid phase reactors R1, R3, R4 there are pillars, located at the entry and exit to prevent the leaking of beads inside the cassette (Fig. 5 and 7d, S1†). Beads for SPE are added without pre-conditioning after molding and bonding of the cassette by the top where a hole is left (Fig. S1†). The hole is sealed at the end of the manufacturing. Mass of beads is dependent on their size but typically is around 25 mg for R1 and R3 chambers and 100 mg for R4.

Each synthesis can use specific beads in reaction chambers and different fluidic structures of the cassette for routing, mixing and dilution of liquids. The reagents and the beads are chosen according to the synthesis process. Therefore, each cassette is intended for the synthesis of a specific radiotracer.

The vials can be positioned in up to 9 positions. The use and the positions of the different vials have to be adapted to the synthesis. Of these 9 positions, 6 correspond to 4 mL (maximal volume) vials (vials A–F) and 3 to 15 mL vials (vials G–I, Fig. 3a). The operating volumes are from few hundreds of μL to several mL. The dead volumes in vials are ≤100 μL

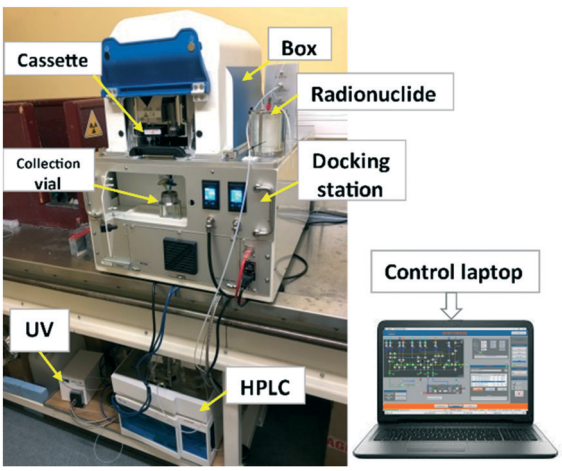

Fig. 2 iMiDEV™ microfluidic platform including the box, docking station, HPLC.

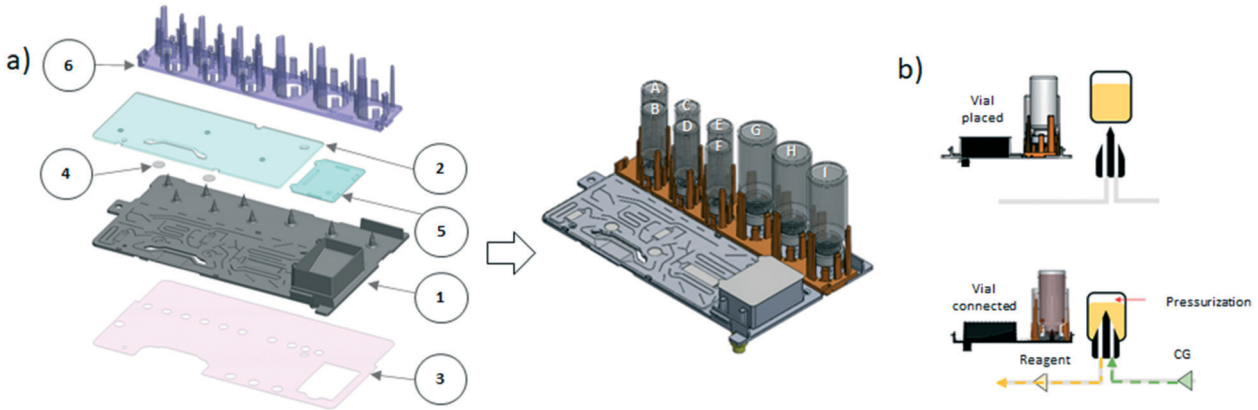

Fig. 3 iMiDEV cassette design: a) 3D cassette representation: 1 – middle COP layer with valves, chambers and spikes for vials; 2 – top COP layer; 3 – bottom COC-E-140 membrane; 4 – hydrophobic filters; 5 – formulation chamber cover; 6 – vial holder; b) vial fluidic connection (clamping) *via* spike with the carrier gas (CG), cassette side view.

and are going to be improved. Formulation chamber has total volume of 12 mL with quite low residual dead volume depending on fluid viscosity.

In radiopharmaceutical production, the cassette is considered as a single use disposable consumable. But, after SPE regeneration, in R&D it can be used several times to test the reliability and repeatability of the process or optimise the synthesis.

2.4 Clamping system

Two clamping mechanisms are supplied by 4 compressed air channels and controlled by solenoid valves of the synthesizer. The first clamping allows the cassette to be pressed onto the docking plate and a second clamping connects the vials placed in the vial holder with the cassette *via* spikes (Fig. S2† and 3b). The cassette clamping insures the correct alignment of the cassette with the pneumatic actuation for the microfluidics valves. Vial clamping can only be activated if cassette clamping is first carried out (corresponding sensors are integrated in the box).

2.5 Software – human–machine interface (HMI)

The software is linked to the control system which communicates with all the electronic equipment of the docking station, the box and the HPLC system (Fig. 1 and 2). Online monitoring can be carried out in the user-friendly layout which displays a production process. Thus, HMI controls all 34 microfluidic valves of the cassette, thermoelectric device (Peltier), HPLC pump, collects the data from sensors (cassette and vials presence, temperature, pressure, optical, UV and radioactivity). At the end of production all raw data are automatically saved. The automation of the synthesis is made by creation of a sequence that can be loaded and monitored from the software. In addition, HMI gives access to three modes of use. The first – manual mode – allows the user to drive each part of the system individually, used by radiochemist for method development and the technical team for the maintenance of the equipment. Then, in a semi-automatic mode, the user must validate each step to proceed to the next, and finally using the automatic mode, the sequence runs until the end of the synthesis.

2.6 Production setup

Before the production, the carrier gas and compressed air pressures and the communication with software have to be verified. Once the system is ready the first part of production process consists of:

1) Placing the vials in the correct order on the vial holder.
2) Cassette positioning in the iMiDEV™ box (Fig. S2†).

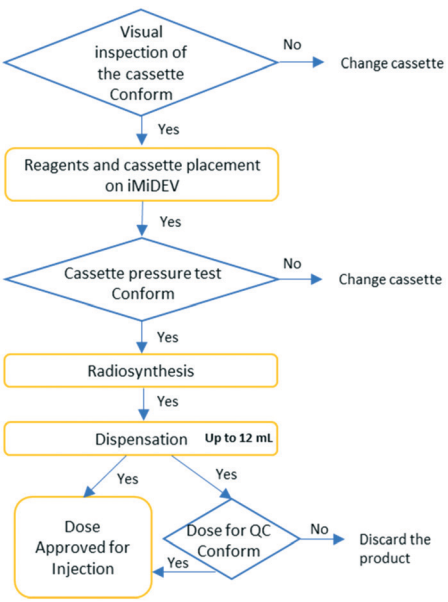

Fig. 4 Flow chart of a single-dose radiopharmaceutical production on iMiDEV™ microfluidic platform.

3) Check the transfer line connection between the box and the radionuclide source.

4) Cassette clamping.

5) Microfluidic radiosynthesis – sequence loading (clamping of vials is actuated automatically) following the correct execution of the activity transfer and all production steps.

Starting point of every synthesis is to close every 34 microfluidic valves, only the necessary ones are opened one by one by releasing the pressure exerted on them during the synthesis. Once the synthetic step is completed the actuated valves are simultaneously closed. For sodium [^{18}]fluoride production two reactors R1 or/and R3 have to be loaded with a quaternary methyl ammonium anion exchange beads (QMA). Single batch preparation can be executed following the same automated process for both reactors. The radiosynthesis is divided into three steps as follows:

- Activity reception: the fluoride-18 solution is transferred into injection port of the cassette.

- Synthesis: the fluoride-18 solution is passed through the corresponding chamber loaded with QMA beads to trap the fluoride-18 and enriched water is eliminated towards waste. The QMA beads in chambers are washed with sterile distilled water of the pharmaceutical grade and then flushed with nitrogen gas flow.

- Delivery: the fluoride-18 is eluted from the QMA beads with 0.9% NaCl and a final pure product is sent from the formulation chamber of the cassette *via* tubing inserted through a syringe port to the collection vial placed in the docking station. Formulated solution is filtered through a sterile Millex-GS filter (0.22 μm) placed before the collection vial. The activity of the prepared [^{18}F]NaF was measured in a radioisotope dose calibrator (CRC®-25R, Capintec, Inc.). The radiochemical yield for sodium [^{18}F]fluoride production was calculated as the ratio of the decay-corrected radioactivity of the final solution collected after elution with normal saline solution, divided by the initial radioactivity of [^{18}F]fluoride introduced into the radiosynthesis process measured by dose calibrator before starting the synthesis. The product was then released for quality control.

2.7 Cerenkov luminescence imaging (CLI)

After the synthesis was completed, the cassette underwent Cerenkov luminescence imaging to check presence and distribution of residual activity. Images were acquired from the top and bottom transparent sides of the cassette. They were acquired on an OptiMAX multimodal imaging device (Precision X-ray Inc., North Brandford, CT). The imaging device consists of a super-cooled optical camera placed into the chamber of an X-RAD 320 preclinical irradiator (Precision X-ray Inc., North Brandford, CT).[35] Cerenkov image was acquired with a 4 minute acquisition duration and an aperture of 0.5. To accurately localize potential foci, a white-light image was also performed for each session to observe the cassette (acquisition duration = 0.5 s, aperture = 0.9). Cerenkov and white-light images were then merged using ImageJ software (Fig. S9 and S10†). White-light images were optimized to provide better visualisation. In all experiments no activity was detected in the microfluidic channels of the bottom part of the cassette therefore only images of the top part are presented hereafter.

2.8 Quality control procedure

The activity measurements were carried out using the radioisotope dose calibrator (CRC®-25R, Capintec, Inc.).

Appearance was determined by visual inspection of the product.

pH of the solution was determined by putting a drop of solution onto a pH indicator strip and comparing the colour on the strip with the provided scale.

Radionuclide purity and identity of [^{18}F]F, were determined by gamma-ray spectrometer (miniGITA, Elysia-Raytest®). Radionuclide identity was confirmed by the time-decay method measured on the dose calibrator (CRC®-25R, Capintec, Inc.).

Radiochemical purity of [^{18}F]NaF was first determined by thin layer chromatography (TLC) on a silica gel as stationary phase eluted with acetonitrile/water (95/5 v/v) using a TLC-scanner (miniGITA, Elysia-Raytest®).

Radiochemical purity and identity were determined by analysing an aliquot of [^{18}F]NaF on high performance liquid chromatography (HPLC) run on a Waters Alliance e2695 system equipped with 2998 photodiode array (PDA) detector and the radio HPLC detector (Herm LB500 with NaI detector, Berthold, Bad Wildbad, Germany) controlled by the Empower Software (Orlando, FL, USA). The column used was a Dionex™ CarboPac™ PA10 (4 × 250 mm) equipped with a suitable precolumn from Thermo Scientific™ and with 0.1 M sodium hydroxide solution at 1 mL min^{-1}.

Sterility and endotoxin tests were carried out on the [^{18}F]NaF samples (post radioactive decay) of each batch according to the European Pharmacopoeia monograph requirements.

Table 1 Comparison of radiolabelling yields and activity losses obtained using different chambers in the single and double productions of [^{18}F]NaF

Entry	Reaction chambers	Number of trials	RCY (dc),[a] %	Residual activity on cassette and collection tubing, %	Activity in the waste, %
1	R1	2	91.9 ± 2.8	8.1 ± 2.8	0
2	R3	7	82.2 ± 5.1	17.4 ± 4.9	0.3 ± 0.3
3	R3/R1	5	82.5 ± 6.1%/90.4 ± 5.3%	17.2 ± 5.9/9.2 ± 5.4	0.3 ± 0.3

[a] RCY (dc) – decay-corrected radiochemical yield.

Sterility was verified by direct inoculation of at least 1 mL of [^{18}F]NaF with resazurin in thioglycollate and trypticase soya media. Culture tubes were incubated at 32.5 °C for resazurin thioglycollate media and 22.5 °C for trypticase soya for 14 days and visually inspected daily.

Analyses of endotoxin content in [^{18}F]NaF were performed using rapid test cartridges for LAL (Endosafe® nexgen-PTS™, Charles Rivers).

2.9 Micro-PET imaging [^{18}F]NaF

A healthy male adult Wistar rat (436 g) was briefly anesthetized by inhalation of isoflurane and intravenously injected with 80 MBq (0.7 mL) of [^{18}F]NaF, 60 minutes prior to initiating PET acquisition. This acquisition was obtained under the same isoflurane anesthesia with a dedicated small-animal PET system (Siemens, Knoxville, USA, Tennessee, USA). The animal was placed in prone position on a heating pad with a recording time of 60 minutes for ^{18}F-emission and 10 minutes for ^{57}Co transmission. Images were reconstructed in a dynamic of 6 frames of 10 min of duration using the ordered-subsets expectation maximization 3D algorithm (OSEM3D) together with scatter and attenuation corrections based on transmission source measurement. The final voxel size was 0.8 × 0.8 × 0.9 mm^3. Two spheroid regions of interest (ROIs) were placed inside the rodent's vertebrae with the ROI limits approximating the vertebrae limits as close as possible. The corresponding volume of interest was applied to the full dynamic data set to generate an activity-time curve. This animal experiment was conducted in accordance with protocols approved by the Lorraine ethics committee N°68 according to guidelines of animal care and use.

3 Results and discussion

The automated module iMiDEV™ was elaborated for the purpose of a single-dose radiopharmaceutical drug production following the flow chart on Fig. 4.

Fluidic and mechanical performances of this new microfluidic platform have been originally tested by the manufacturer including flow parameters of different reagents, material compatibility validation of the cassette and repeatability of the system.

Implementation of radiochemistry on this new synthesizer was tested in partnership with Nancyclotep (France) and Karolinska Institutet (Sweden) in order to validate the performance of iMiDEV™.

The production of [^{18}F]NaF was successfully adapted to the microfluidic cassette-based iMiDEV™ system. The specific cassettes (next NaF-cassette, Fig. 3) were fabricated with R1 and R3 chambers packed with quaternary methyl ammonium strong anion exchange beads in chloride form (QMA-Cl, 24 mg, 37–55 μm, Waters®, hold up chamber volume 50 μL) to enable the trapping and concentration of ^{18}F-fluoride. Fluid circuit was adjusted by using valves and directing reagent delivery in microfluidic network. The gas control system provided a carrier gas flow necessary for vials pressurisation and for liquid movement.

3.1 Automation of [^{18}F]NaF radiosynthesis on iMiDEV cassette

In the case of production through R1, vial containing 1 mL of sterile distilled water was installed on position A and a second vial containing 5 mL of NaCl 0.9% was placed on position G (Fig. 4). The production was fully automated by creating the sequence with all actions necessary to perform the three steps described as follows (Fig. S3†). Firstly, the aqueous [^{18}F]fluoride was transferred from an external container through the isotope port to the chamber R1 of the cassette by opening microfluidic valves 6 and 3 (using a nitrogen gas flow at 1 bar for 2 min). ^{18}O-enriched water was collected through the waste port while fluoride-18 was retained on the QMA-Cl beads. Duration of [^{18}F]fluoride trapping on QMA in R1 varied from 25 s to 1.5 min

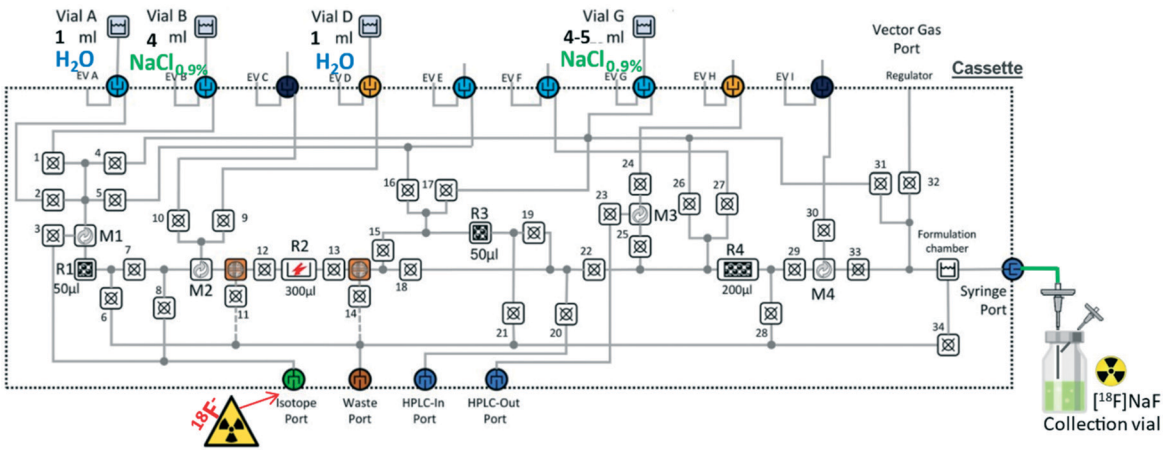

Fig. 5 Schematic of the microfluidic cassette configuration for [^{18}F]NaF synthesis; single in R1: vials A and G; single with R3: vials D and G; double: vials D and G for production using R3 and vials A and B while using R1; R1–R4 – reactors, M1–M4 – mixers, EVA – EVI – electrovalves, 1–34 – microfluidic valves.

depending on the [^{18}F]fluoride dilution (V = 0.6–3 mL, Fig. 6). The next step consisted of washing the QMA solid phase with sterile distilled water (vial A, 1 mL, by opening microfluidic valves 6 and 2 towards the waste port using nitrogen gas at 1 bar for 2 min). Lastly, sodium [^{18}F]fluoride was formed by passing 0.9% NaCl solution through R1 chamber (vial G, 5 mL, by opening microfluidic valves 33, 29, 22, 18, 13, 12, 7 and 4 towards the formulation chamber using nitrogen gas at 1.5 bar for 3 min). Produced [^{18}F]NaF was eluted in one portion from the formulation chamber and the syringe port through a sterile filter to the collection vial. All parameters and specific operations where configurated through the software.

Trap-release process was monitored with PIN diode radiation detectors (Fig. 6) present in the box to control the radiotracer production.

3.2 Optimisation of [^{18}F]NaF radiosynthesis

Several parameters such as a different type of cyclotron targets, initial radioactivity, concentration and volume of the F-18 ion were tested to optimise synthesis method, total synthesis time, and to achieve maximum yield. Only one cassette (reactivated by 0.9% NaCl) with R1 and R3 reaction chambers was used in the research of optimised parameters for production of [^{18}F]NaF.

Target. Two distinct types of silver and niobium targets for the production of [^{18}F]F$^-$ were used in order to test the influence of the target on the yield of [^{18}F]NaF as the silver target has more metal ion impurities than niobium target. The volume of [^{18}O]water used for silver target was 1,5 mL and for niobium target was 2.5 mL. Our study showed there was no significant difference in the yield of [^{18}F]NaF using two different targets (85.8 ± 1.3% (n = 4) for silver target and 80.3 ± 8.2% (n = 12) in case of niobium target, Table S2†).

Initial radioactivity. We tested initial radioactivity from 122 MBq to 1609 MBq to evaluate the yield of produced [^{18}F]NaF. Our result showed that initial radioactivity up to 1609 MBq does not affect the yield of [^{18}F]NaF if the volume and concentration of the F-18 ion were maintained accordingly (Table S2†).

Concentration of initial radioactivity. Different radioactive concentration of fluoride-18 from 49 to 1073 MBq mL^{-1} were tested to evaluate the produced yield of [^{18}F]NaF comparing with initial radioactivity used for synthesis. We observed that when the concentration of [^{18}F]F$^-$ was higher, the loss of radioactivity ([^{18}F]F$^-$) in the cassette and isotope transfer tubing was greater. On the contrary, less activity was lost when the starting F-18 concentration was lower (Fig. S4†). In our investigation, we found that an initial concentration of radioactivity lower than 250 MBq mL^{-1} leads to highest [^{18}F]NaF yields (Fig. S4†).

Volume of fluoride-18. We tested the initial [^{18}F]F$^-$ volume range from 0.45 mL to 3.3 mL, and have identified that the volume of the starting activity is one of the main parameters which is affecting the radiochemical yield. Our experimental results showed that when the volume of the initial radioactivity is more than 1.5 mL it helps to achieve maximum yield of [^{18}F]NaF. The average yield of 87 ± 2% (n = 8) was observed when we used 1.5–3.3 mL of the water solution of fluoride-18 (Fig. S5†).

Once the initial parameters like initial radioactivity of [^{18}F]F$^-$, its concentration and volume have been found we proceeded to the validation of fully automated [^{18}F]NaF production using a new cassette for each run.

3.3 Production of injectable [^{18}F]NaF

For single radiosynthesis, only one chamber R1 or R3 was used. Typical [^{18}F]NaF synthesis started with around 165 MBq of [^{18}F]fluoride in 1–2 mL of a proton beam-irradiated water target and produced in the average of 150 MBq of [^{18}F]NaF. In view of [^{18}F]NaF radiopharmaceutical production guidelines, it is necessary to inject 185–370 MBq to patient to acquire a bone PET-scan.[36] Therefore a low activity synthesis was investigated as it is the main purpose of iMiLAB™ robotized system which is single-dose tracer production and uses the same microfluidic cassette and synthesizer. Trapping efficiency was evaluated by measuring activity of the [^{18}O]H_2O recovered from the vial connected to the waste port of the cassette during the first step and was shown to be more than 99%. Using 25 mg QMA-Cl integrated resin allowed us to reach a concentration of ^{18}F- around 3 GBq mL^{-1} within 50 μL reactor. The time necessary to release the concentrated radioactivity did not exceed 15 s. Therefore in a single production using R1 chamber, [^{18}F]NaF was obtained in 91.9 ± 2.8% radiochemical yield (dc, Table 1). Production time in the automatic mode of the sequence execution was 8 min.

Following the same procedure [^{18}F]NaF synthesis was successfully transposed to the R3 chamber. In this case vial with distilled water (1 mL) was placed on the position D and the vial with 5 mL of normal saline was placed on the position G (Fig. 5). Identical time–pressure parameters were applied for fluid transfer. Technical implementation of all steps is schematically described in Fig. S6.† Trapping-releasing efficiency was measured in the same manner as for R1 and was quantitative (Fig. S7†). Thus, the product was

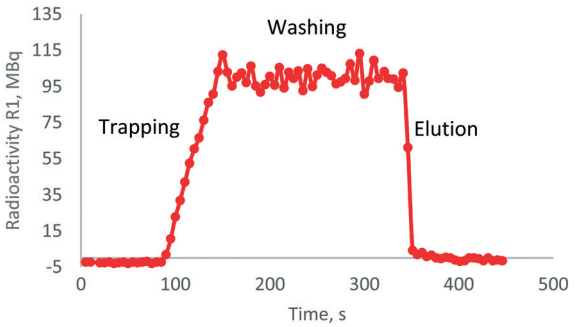

Fig. 6 Trap-release radioactivity curve obtained after [^{18}F]NaF synthesis on R1 chamber; activity was concentrated from 2 mL of irradiated target [^{18}F]fluoride solution.

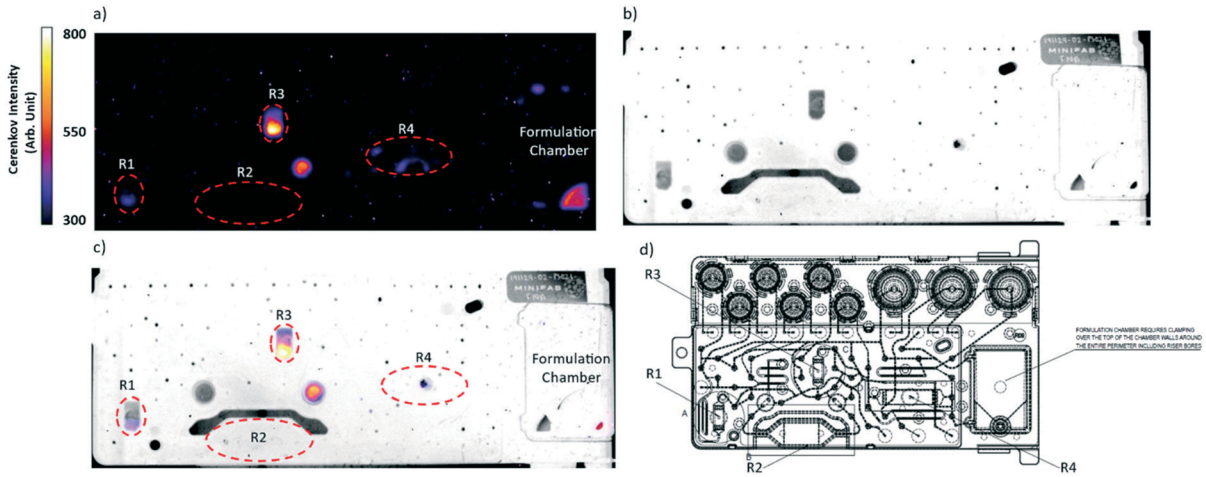

Fig. 7 Cerenkov imaging of the residual activity distribution on the cassette after two consecutive productions of sodium [^{18}F]fluoride on R3 and R1 chambers: a) Cerenkov image after synthesis; b) white-light image of the top of the cassette; c) merged Cerenkov and white-light images after completion of the synthesis; d) schematic location of microreactors on the cassette, top view.

obtained in 82.2 ± 5.1% radiochemical yield (dc, Table 1) during 8 min. Considering that the cassette provides sufficient number of vials and reactors to be applied, double synthesis was performed on R3 and R1 without any reagent or cassette reloading. Vials containing 1 mL of sterile distilled water were installed on the positions A and D and vials with 4 mL of NaCl 0.9% were placed on the positions B and G (Fig. 5). Reagent transfer to the cassette was achieved by applying the same conditions described above for the single run. Both R3 and R1 QMA-chloride filled μ-cartridges have been consecutively implemented in the syntheses. Microfluidic valve network that is related to this delivery of reagents is showed in Fig. S8.† However such double-batch production needs human intervention for placing a new source of [^{18}F]fluoride and the final product vial after the first batch delivery is completed. Though the sequence was loaded in the automatic mode a special "wait" step should be added to temporarily stop the latter until the operator action permitted to continue the process. The overall production time of two batches in the automatic mode of the sequence execution was around 17 min. The radiochemical yields were measured for every production run and were 90.4 ± 5.3% when using R1 and 82.5 ± 6.1% on R3 chamber (Table 1). They were comparable to yields obtained on conventional macroscale modules (>90%).[32,37] The activity losses measured in the waste after isotope trapping and QMA rinsing of R1 and R3 were negligible (Table 1). The difference in yields obtained using R1 or R3 in single or double synthesis therefore comes from the higher residual activity on cassette and collection tubing when microfluidic network containing R3 is used (Table 1). To find out the activity loss limitation step we decided to compare the way that passes F-18 isotope during trapping and elution steps. From this comparison we may observe that before being trapped on R3 the liquid passes the reaction chamber R2 with a big dead volume while in case of R1 the liquid is injected directly on the beads. This led us to suggest that the major activity loss occurs during the activity injection step. To confirm our hypothesis a Cerenkov luminescence imaging (CLI) technique was used to visualize the distribution of residual activity after trapping and collection steps. Thus, Cerenkov experiments were performed for synthesis on R3. Indeed, the residual activity was found in R2 reactor after loading of nuclide was completed (Fig. S9†). CLI after [^{18}F]NaF synthesis on R1

Table 2 Quality control (QC) test data summary for three batches of [^{18}F]NaF on R1 and R3

Trial	Quality requirements	Validation run 1	Validation run 2	Validation run 3
Appearance	Clear, colorless, free of particulates	Complies	Complies	Complies
pH	5–8.5	5.6	5.6	5.6
Radiochemical identity	RRT[a] = 0.9–1.1	1.0	1.0	1.0
Radiochemical purity	>98.5% by HPLC	Complies	Complies	Complies
Radionuclidic identity	$T_{1/2}$[b] = 105–115 min	107	109	112
	Emission 511 keV ± 10%	511	518	518
Radionuclidic purity	>99.9%	Complies	Complies	Complies
Bacterial endotoxin	<175 EU[c] per dose	3.97	6.6	72.5
Sterility	Sterile	Sterile	Sterile	Sterile

[a] Relative retention time (RRT = [retention time of fluoride-18]/[retention time of fluoride- 19]), rounded to the nearest 1/10. [b] Semi-disintegration period. [c] Endotoxin units.

showed that residual activity stays trapped in the beginning of the chamber R1 (Fig. S10†). Finally, CLI combined with a white-light image after a double synthesis experiment on a new cassette presented in Fig. 7.[38,39] The residual activity on cassette and collection tubing in representative experiment was 23.6% after the synthesis on R3 and 3.8% after the labelling on R1. Interestingly, some activity stays trapped in one of the hydrophobic filter where the activity could not be efficiently recovered during product collection (Fig. 7). Due to the dead volumes some drops can also be observed in R4 and formulation chamber. However, from the image we could observe that the maximum activity loss within the cassette occurs in R3 chamber. This last fact explains the difference in radiochemical yields obtained using both reactors. Therefore, for a single production it is preferable to utilize R1 reactor with minimal product losses.

3.4 Quality control

Quality control of this radiopharmaceutical ([^{18}F]NaF) was performed according to the most recent European Pharmacopoeia (Eur. Pharm.) requirements.[33] Quality control was performed on an aliquot of [^{18}F]NaF. The prepared radiopharmaceutical solution was clear and colourless with a pH around 5.6. Radionuclide identity that was determined by the consecutive half-life measurements (10 min intervals) was confirmed by a half-life of 109 ± 2 min and gamma emission at 511 keV. Radionuclide purity that was determined by gamma-ray spectrophotometer showed the presence of one radionuclide with the energy of 511 keV (Fig. S11†). After decay no long-lived radionuclide contaminants were identified. High performance liquid chromatography (HPLC) of [^{18}F]NaF after 1 h of column conditioning with mobile phase at 1 mL mL^{-1} showed a retention time in the range of 4.5–4.8 min with radioactive detection according to the Eur. Pharm. monograph (Fig. S12†). The radiochemical purity determined by HPLC and radio-TLC methods was up to 99.99%. The UV-HPLC chromatogram of [^{18}F]NaF had no UV detectable amount present.

Sterility and endotoxin tests showed a good biological purity of our radiopharmaceuticals.

A summary of data collected for three repeated batches is reported in Table 2.

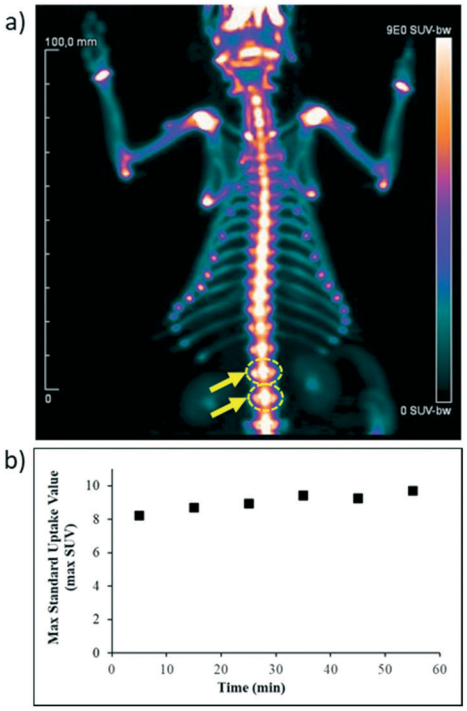

Fig. 8 (a) Summed PET image recorded during 60 min, 1 hour following injection of [^{18}F]NaF prepared on iMiDEV™ in one healthy rat. Colour scale is expressed in SUV values. (b) Corresponding activity-time curve for maxSUV from vertebrae obtained during 60 min of acquisition (black square).

3.5 Micro-PET imaging [^{18}F]NaF

To validate the quality of the [^{18}F]NaF synthesized on iMiDEV™ cassette, the *in vivo* biodistribution was studied by imaging a healthy male rat. As shown in Fig. 8, the image of the rat exhibits the expected homogeneous skeletal uptake of the radiotracer.

Analysis of the [^{18}F]NaF uptake performed by determining maxSUV (maximal standard uptake value) within 3D ROI, drawn with a dedicated software in vertebrae (yellow arrows). We observe the maxSUV values ranging from 9 to 10.50 for [^{18}F]NaF produced on iMiDEV™. These values correspond to a high uptake of [^{18}F]NaF similar to those observed in clinical routine and the value remains stable over time during the 60 min of acquisition.

4 Conclusions

In conclusion, iMiDEV™ synthesizer based on microfluidic cassette was shown to be able to produce radiopharmaceutical with a straightforward method. Rapid single or double-batch production of sodium [^{18}F]fluoride using a new microfluidic on-cassette platform is presented. The fluoride-18 concentration up to 1.6 GBq has shown to be easily accomplished *via* an integrated miniaturised anion exchange cartridge. Its capacity can also be used to scale-up the microfluidic tracer production and the activity limit will be determined in the near future.

From a preliminary study it was also determined that the initial [^{18}F]F$^-$ concentration has to be less than 250 MBq mL^{-1} and the volume is more than 1.5 mL in order to attain the highest yields. Sodium [^{18}F]fluoride was synthesised in up to 92% decay-corrected radiochemical yield within 8 min production. The advantage of the new cassette is the opportunity to carry out two consecutive [^{18}F]NaF syntheses without the need of changing reagents or manipulating the cassette. In general, the iMiDEV™ system seems to provide a good opportunity for single-dose or small-scale radiopharmaceutical production. This proof of concept showed that iMiDEV™ module can be used for routine cGMP production of [^{18}F]NaF for PET-scan diagnosis imaging in

realising 3 consecutive batches which conform to quality control according to Eur. Pharm. This versatile system potentially could also be used to perform multistep syntheses of radiopharmaceuticals with benefits from preconcentration technology, small-volume and rapid fluid and heat transfer.

Conflicts of interest

There are no conflicts to declare.

Acknowledgements

The authors would like to thank Dr. Laurent Tanguy and Yahya Cisse for their support and assistance regarding technical issues concerning the iMiDEV™ system. We also thank Dr. Joël Daouk for assisting with Cerenkov luminescence imaging. We gratefully acknowledge the financial support for this research by the following organizations: Great East European Regional Development Fund (ERDF) and Contrat Plan Etat-Région (CPER) from French government and Great East Regional Council.

References

1 M. P. S. Dunphy and J. S. Lewis, *J. Nucl. Med.*, 2009, **50**, 106S–121S.
2 M. Piel, I. Vernaleken and F. Rösch, *J. Med. Chem.*, 2014, **57**, 9232–9258.
3 H. Audrain, *Angew. Chem., Int. Ed.*, 2007, **46**, 1772–1775.
4 R. Fortt and A. D. Gee, *Future Med. Chem.*, 2013, **5**, 241–244.
5 C. Rensch, A. Jackson, S. Lindner, R. Salvamoser, V. Samper, S. Riese, P. Bartenstein, C. Wängler and B. Wängler, *Molecules*, 2013, **18**, 7930–7956.
6 K. Knapp, M. L. Nickels and H. C. Manning, *Mol. Imaging Biol.*, 2020, **22**, 463–475.
7 M.-W. Wang, W.-Y. Lin, K. Liu, M. Masterman-Smith and C. K.-F. Shen, *Mol. Imaging*, 2010, **9**, 175–191.
8 P.-Y. Keng, M. Esterby and R. M. van Dam, Emerging technologies for decentralized production of PET tracers, in *Positron emission tomography - current clinical and research aspects*, ed. C.-H. Hsieh, InTech, Rijeka, 2012, pp. 153–182.
9 G. Pascali, P. Watts and P. A. Salvadori, *Nucl. Med. Biol.*, 2013, **40**, 776–787.
10 P. W. Miller, *J. Chem. Technol. Biotechnol.*, 2009, **84**, 309–315.
11 S. Haroun, Z. Sanei, S. Jivan, P. Schaffer, T. J. Ruth and P. C. H. Li, *Can. J. Chem.*, 2013, **91**, 326–332.
12 S. Haroun, L. Wang, T. J. Ruth and P. C. H. Li, *Chem. Eng. Process.*, 2013, **70**, 140–147.
13 V. Arima, G. Pascali, O. Lade, H. R. Kretschmer, I. Bernsdorf, V. Hammond, P. Watts, F. de Leonardis, M. D. Tarn, N. Pamme, B. Z. Cvetkovic, P. S. Dittrich, N. Vasovic, R. Duane, A. Jaksic, A. Zacheo, A. Zizzari, L. Marra, E. Perrone, P. A. Salvadori and R. Rinaldi, *Lab Chip*, 2013, **13**, 2328–2336.
14 S.-Y. Lu, P. Watts, F. T. Chin, J. Hong, J. L. Musachio, E. Briard and V. W. Pike, *Lab Chip*, 2004, **4**, 523–525.
15 S.-Y. Lu, A. M. Giamis and V. W. Pike, *Curr. Radiopharm.*, 2009, **2**, 49–55.
16 L. Matesic, A. Kallinen, I. Greguric and G. Pascali, *Nucl. Med. Biol.*, 2017, **52**, 24–31.
17 C.-C. Lee, G. Sui, A. M. Elizarov, C. J. Shu, Y. S. Shin, A. N. Dooley, J. Huang, A. Daridon, P. Wyatt, D. Stout, H. C. Kolb, O. N. Witte, N. Satyamurthy, J. R. Heath, M. E. Phelps, S. R. Quake and H. R. Tseng, *Science*, 2005, **310**, 1793–1796.
18 D. L. Yokell, A. K. Leece, A. Lebedev, R. Miraghaie, C. E. Ball, J. Zhang, H. Kolb, A. Elizarov and U. Mahmood, *Appl. Radiat. Isot.*, 2012, **70**, 2313–2316.
19 X. Zhang, F. Liu, K.-A. Knapp, M. L. Nickels, H. C. Manning and L. M. Bellan, *Lab Chip*, 2018, **18**, 1369–1377.
20 P.-Y. Keng and R. M. van Dam, *Mol. Imaging*, 2015, **14**, 13–14.
21 H. Wang, L. Chen and L. Sun, *Front. Mech. Eng.*, 2017, **12**, 510–525.
22 J. Wang, P. H. Chao, S. Hanet and R. M. van Dam, *Lab Chip*, 2017, **17**, 4342–4355.
23 C. Frank, G. Winter, F. V. Rensei, V. Samper, B. G. Hockley, B. D. Henderson, C. Rensch and P. J. H. Scott, *EJNMMI radiopharm. chem.*, 2019, **4**(24), 1–18.
24 S. A. Fiel, H. Yang, P. Schaffer, S. Weng, J. A. H. Inkster, M. C. K. Wong and P. C. H. Li, *ACS Appl. Mater. Interfaces*, 2015, **7**, 12923–12929.
25 F. de Leonardis, G. Pascali, P. A. Salvadori, P. Watts and N. Pamme, Microfluidic modules for [$^{18}F^-$] activation - Towards an integrated modular lab on a chip for pet radiotracer synthesis, *14th International Conference on Miniaturized, Systems for Chemistry and Life Sciences, MicroTAS*, 2010, 3, 1604–1606.
26 B. Salvador, A. Luque, L. Fernandez-Maza, A. Corral, D. Orta, I. Fernandez and J. M. Quero, *J. Microelectromech. Syst.*, 2017, **26**, 1442–1448.
27 S. Lu, J. T. Clements, M. J. Gilde, A. Prak, P. Watts and V. W. Pike, *J. Labelled Compd. Radiopharm.*, 2007, **50**, 597–599.
28 W.-Y. Tseng, J. Cho, X. Ma, A. G. Kunihiro, A. Chatziioannou and R. M. van Dam, Toward reliable synthesis of radiotracers for positron emission tomography in PDMS microfluidic chips: study and optimization of the [18F] fluoride drying process, NSTI Nanotechnol. Conf. Expo, 2010, 2, 472–475.
29 X. Zhang, F. Liu, A. C. Payne, M. L. Nickels, L. M. Bellan and H. C. Manning, *Mol. Imaging Biol.*, 2020, **22**, 1370–1379.
30 M. Blau, R. Ganatra and M. A. Bender, *Semin. Nucl. Med.*, 1972, **2**, 31–37.
31 K. Kairemo and H. A. Macapinlac, *Sodium Fluoride PET/CT in Clinical Use*, Springer, Cham, 2019, DOI: 10.1007/978-3-030-23577-2.
32 C. Collet, M. Otabashi, F. Giacomelli, N. Veran, G. Karcher, Y. Chapleur and S. Lamandé-Langle, *Appl. Radiat. Isot.*, 2015, **102**, 87–92.
33 Sodium Fluoride (18F) Injection, European Pharmacopoeia, 10th edn, 2020.
34 V. Hourtane, L. Tanguy and F. Pineda, Microfluidic cassette for synthesising a radiotracer and method for synthesising a

radio-tracer with such a cassette, WO2019077238, 2019, CAN170:53725.

35 J. Daouk, J. Jubréaux, A. Chateau, H. Schohn and S. Pinel, *Clinical Oncology & Research*, 2020, **3**(2), 1–4.

36 G. Segall, D. Delbeke, M. G. Stabin, E. Even-Sapir, J. Fair, R. Sajdak and G. T. Smith, *J. Nucl. Med.*, 2010, **51**, 1813–1820.

37 B. G. Hockley and P. J. H. Scott, *Appl. Radiat. Isot.*, 2010, **68**, 117–119.

38 A. A. Dooraghi, P. Y. Keng, S. Chen, M. R. Javed, C.-J. Kim, A. F. Chatziioannou and R. M. van Dam, *Analyst*, 2013, **138**(19), 5654–5664.

39 J. Wang, P. H. Chao and R. M. van Dam, *Lab Chip*, 2019, **19**, 2415–2424.